JPPIPA 12(5) (2026)

Jurnal Penelitian Pendidikan IPA

http://jppipa.unram.ac.id/index.php/jppipa/index

Proof-of-Concept of Chitosan–Cellulose Composite Filters for Microplastic Removal from Wastewater

Rizki S. Titisari[1,2,*], Daffa Hifrizi[1], Laily Isrofiani[1], Sapto P. Putro[1,2], Samuel Andre Yulianto[3], Farrel Rahman Parwoto[3], Andya Setya P. Putro[3]

[1] Department of Biology, Faculty of Science and Mathematics, Universitas Diponegoro. Jl. H. Prof. Soedarto, SH., Semarang 50275, Central Java, Indonesia
[2] Center of Marine Ecology and Biomonitoring for Sustainable Aquaculture, Diponegoro University 50275, Tembalang, Semarang, Central Java, Indonesia.
[3] SMA Semesta Bilingual Boarding School 50229, Semarang, Central Java, Indonesia.

Received: January 18, 2026
Revised: Apri 07, 2026
Accepted: May 25, 2026
Published: May 31, 2026

Corresponding Author:
Rizki S. Titisari
rizkisandhi@live.undip.ac.id

DOI: 10.29303/jppipa.v12i5.14315

Open Access

© 2026 The Authors. This article is distributed under a (CC-BY License)

Abstract: Microplastics persist in aquatic systems and are difficult to remove using conventional filtration methods, prompting the development of low-cost, bio-based alternatives. This study presents a proof-of-concept chitosan filter derived from shrimp-shell waste, evaluated as a membrane sheet and as a coating on cellulose filter papers. FTIR confirmed chitosan formation, showing characteristic –OH/–NH stretching (~3450 cm^{-1}), amide I (~1650 cm^{-1}), amide II (~1570 cm^{-1}), and polysaccharide fingerprint peaks (1200–1000 cm^{-1}). Filtration experiments used a fixed 50 mL mixed-microplastic suspension processed under vacuum through five media: chitosan membrane, coffee filter paper, Whatman No. 42, and their chitosan-coated variants. Filtration time was recorded to derive the apparent filtration rate, and retained residues were assessed by visual inspection, stereomicroscopy, and morphometric size measurements in Fiji (particle size range reported as projected digital measurements). Coffee-based media exhibited the highest throughput (>50 mL/min), the chitosan membrane showed intermediate throughput (10 mL/min), and Whatman-based media were the slowest (7.14 mL/min). Chitosan-containing media displayed localized deposition and broader retained size ranges (up to 3.5 µm) compared with uncoated cellulose. Overall, the results support a waste-to-resource chitosan filtration approach that adds surface-mediated retention alongside passive sieving, with promising potential for application in laboratory-scale and pilot-scale wastewater treatment systems.

Keywords: Bio-based filtration; Chitosan; FTIR characterization; Microplastic; Shrimp shell waste

Introduction

Plastic pollution in aquatic environments represents a significant global concern because of its persistence, ubiquity, and the associated risks to both ecosystems and human health (Davis and Raja, 2020). Larger plastic debris undergoes physical and chemical degradation, resulting in the formation of microplastics, defined as plastic particles smaller than 5 mm. Microplastics exhibit resistance to natural degradation and are conveyed through rivers, home effluents, and industrial wastewater (Karbalaei et al., 2018). Within aquatic systems, microplastics are ingested by a range of organisms, accumulate in biological tissues, and transfer through food webs, ultimately reaching humans and presenting health risks (Badawi et al., 2025). Additionally, microplastics adsorb hazardous substances, including heavy metals and persistent organic pollutants, which may enhance toxic effects and contribute to health problems such as inflammation, oxidative stress, and organ damage (Nawaz et al., 2025; Sethia et al., 2024).

Despite the rise in research on microplastic extraction from water, considerable technological

How to Cite:
Titisari, R. S., Hifrizi, D., Isrofiani, L., Putro, S. P., Yulianto, S. A., Parwoto, F. R., & Putro, A. S. P. (2026). Proof-of-Concept of Chitosan–Cellulose Composite Filters for Microplastic Removal from Wastewater. *Jurnal Penelitian Pendidikan IPA*, *12*(5), 853–862. https://doi.org/10.29303/jppipa.v12i5.14315

obstacles remain due to the diminutive size, structural variability, and biodegradation resistance of microplastics (Uogintė et al., 2022). Conventional treatment processes, such as sedimentation and filtration, often exhibit limited efficiency, especially for smaller microplastics or under variable operational conditions (Kamani et al., 2024). These challenges highlight the necessity for innovative filtration strategies that are selective, efficient, and environmentally sustainable, and that can function as pre-treatment or modular filtration units (Sanjeev and Manjunath, 2025). Bio-based materials have therefore attracted considerable interest as alternatives, as they rely on renewable resources and have reduced environmental impacts (Rajendran et al., 2025).

Chitosan, a cationic biopolymer derived from the deacetylation of chitin in seafood-processing residues such as shrimp shells, has attracted significant interest due to its abundance and favorable physicochemical properties (Lapointe et al., 2020; Wang et al., 2025). The combination of amino and hydroxyl functional groups allows for significant interactions with suspended particles, making it useful as a natural coagulant or flocculant in water purification procedures (Bavel et al., 2023). These properties indicate that chitosan may facilitate microplastic removal through mechanical filtration, electrostatic attraction, and floc-mediated retention mechanisms (Picos-Corrales et al., 2020). Although the efficacy of chitosan in eliminating turbidity, heavy metals, and organic contaminants is well established, investigations into chitosan–cellulose composite filters as a floc-filtration mechanism for microplastic extraction, especially under regulated wastewater conditions, remains limited (Badawi et al., 2025; Thathsarani et al., 2025).

This study presents a novel bio-based filtration platform that combines the co-flocculation potential of shrimp-shell-derived chitosan with the mechanical strength of cellulose, establishing a proof-of-concept for microplastic removal from wastewater. The fabricated filters were characterized for structural properties and evaluated under controlled conditions to determine filtration performance and microplastic retention efficiency. This approach addresses the urgent demand for sustainable, cost-effective microplastic removal technologies and offers a scalable solution for wastewater treatment.

Method

Time and Place

The research was conducted from October 2025 to January 2026. Synthesis and preliminary performance testing of the Chitosan Floc-Filter took place at the Center of Marine Ecology and Biomonitoring for Sustainable Aquaculture (Ce-MEBSA) Laboratory, Diponegoro University, Semarang. Physicochemical characterization of chitosan was carried out at the Physics Laboratory, Universitas Negeri Semarang.

Materials and Equipments

Shrimp shell waste sourced from local fisheries was used as the primary feedstock for chitin and chitosan synthesis. Processing involved analytical grade sodium hydroxide (NaOH, Emsure® Merck) and hydrochloric acid (HCl, Emsure® Merck), and chitosan was dissolved in a 1% acetic acid solution. Coffee filter paper and Whatman No. 42 filter paper were selected for filter fabrication. For filter performance testing, pure plastic pellets (PET, PP, ABS, HDPE) from primary plastic stores served as standardized microplastic simulants, and these were supplemented with natural microplastic-containing river water samples. Deionized water (conductivity <1 µS/cm) was consistently used for washing, dilution, and experimental rinsing.

Standard laboratory glassware (Pyrex®, UK) including beakers, stirring rods, measuring cylinders, and droppers; disposable Petri dishes (OneLab®, Indonesia); analytical balance (Ohaus Pioneer PA214C, USA); oven; grinder; vacuum pump filter system (Rocker 300-MF31, Taiwan); Hotplate and Magnetic stirrer (Thermo Scientific, USA); stereomicroscope (Nikon SMZ25, Japan); binocular light microscope (Olympus CX21, Japan). pH adjustments and measurements were conducted using a Mediatech pH meter (South Korea) with standard buffer solutions.

Procedure

Preparation of Shrimp Shell Raw Material

Shrimp shell waste was thoroughly washed under running water to eliminate residual flesh and impurities. The purified shells were desiccated in an oven at 60 °C until completely dehydrated, then pulverized into a fine powder for further chemical processing.

Deproteinization

The chitin precursor was produced by deproteinizing shrimp shell powder with 1 N NaOH solution at a solid-to-liquid ratio of 1:4 (g powder/ml NaOH). The suspension was heated at 60 °C for 30 minutes with continuous stirring at 750 rpm. Following treatment, the mixture was filtered, and the solid fraction was washed repeatedly with distilled water until a neutral pH was achieved. The solid was then dried in an oven at 100 °C for 24 hours.

Demineralization

The dried, deproteinized solid underwent demineralization by immersion in 1 N HCl solution,

followed by heating at 60 °C for 30 minutes with stirring at 750 rpm. The suspension was filtered, and the solid residue was rinsed with distilled water until a neutral pH was reached. The material was then dried in an oven at 100 °C for 24 hours to yield dry chitin.

Deacetylation

Chitin was converted to chitosan through deacetylation using 80% NaOH solution. The chitin was immersed in the NaOH solution, then heated and stirred at 60 °C for 60 minutes at 750 rpm. The mixture was filtered, and the solid phase was washed with distilled water until a neutral pH was achieved. The final solid was dried in an oven at 100 °C for 24 hours to obtain chitosan.

Chitosan Characterization

Chitosan samples were analyzed using Fourier Transform Infrared (FTIR) spectroscopy to identify characteristic functional groups and determine the degree of deacetylation (DD). The presence of amide groups (1650-1660 cm^{-1}, C=O stretching) from residual chitin and amine groups (3300-3500 cm^{-1}, N-H/O-H stretching) from chitosan were specifically targeted. The degree of deacetylation was calculated using the standard FTIR method based on the ratio of amide I (1655 cm^{-1}) to amide II (1560 cm^{-1}) peak intensities according to the equation:

$$DD\ (\%) = 100 \times [1 - (A_{1560}/A_{1655})/(A_{1560}/A_{1655})_{kitin}] \quad (1)$$

Spectra were recorded in the range 4000-500 cm^{-1} with 32 scans at 4 cm^{-1} resolution using KBr pellet technique.

Chitosan Filter Fabrication

Five grams (5 g) of synthesized chitosan powder were dissolved in 1% acetic acid using a hotplate magnetic stirrer (750 rpm, 60 °C) until fully homogenized, then 15 mL aliquots were cast into Petri dishes and oven-dried at 60 °C for 60 minutes to form thin polymeric films, which were coagulated by immersion in 0.1 M NaOH for 10 minutes, rinsed with deionized water to neutral pH, and dried at 60 °C for 10 minutes to produce flexible chitosan filter sheets. Chitosan filter sheets were visually characterized by five independent observers to assess flexibility, uniformity, and structural integrity prior to performance testing.

Preparation of Microplastic Test Suspension

Plastic pellets composed of PVC, ABS, PET, and HDPE were pulverized using a grinder to produce microplastic particles. Final particle sizes were estimated from projected digital measurements using Fiji image analysis software on stereomicroscope images: PVC (0.12–10 µm), ABS (0.14–9 µm), PET (0.1–9 µm), and HDPE (0.1–15 µm). Minimum values represent the smallest projected dimensions detectable within the image frame and should be interpreted as digital projections rather than absolute particle sizes. For each microplastic type, 5 g was suspended in 1.5 L of deionized water to create a standardized test matrix, resulting in a total of 20 g microplastics in 1.5 L (13.3 g/L concentration). This elevated concentration simulates highly contaminated industrial wastewater conditions, as reported in filtration performance studies, and facilitates clear differentiation between filter types (Napi et al., 2023; Talvitie et al., 2017). The suspension was homogenized using a magnetic stirrer at 750 rpm for 10 minutes to ensure uniform particle distribution before filtration testing.

Filtration Performance Testing

Microplastic test suspensions were filtered through chitosan-based filter sheets. Uncoated coffee filter paper and Whatman No. 42, along with their chitosan-coated variants, were used as comparative controls. Vacuum-assisted filtration was performed using a Rocker 300-MF31 system, and filtration time was recorded for a fixed volume per run to derive the apparent filtration rate. Each condition was tested in duplicate. Retained residues were examined using a stereomicroscope (Nikon SMZ25, 50–100×), with observations made across five standardized fields of view per sample. Post-filtration, all filter media were visually evaluated by five observers using a predefined 1–5 scoring rubric for physical integrity, flexibility, and surface deposition to assess chitosan-specific contributions to filtration behavior.

Data Analysis

Descriptive-comparative methods were employed to evaluate the feasibility of shrimp shell-derived chitosan as a microplastic filtration medium. FTIR analysis confirmed the presence of characteristic chitosan functional groups, verifying material identity and active sites. Filtration rate (mL/min, calculated as 50 mL divided by filtration time) was measured to assess flow resistance across different media types. Retention patterns were examined both macroscopically (deposit distribution) and microscopically using a Nikon SMZ25 microscope. Fiji software was used to quantify the size range (minimum to maximum, µm) of retained particles across treatments.

Result and Discussion

FTIR Characterization of Extracted Chitosan

FTIR analysis demonstrated that the shrimp shell waste extract displayed absorption bands matching stablished chitosan spectral signatures (Table 1). The

broad band at approximately 3450 cm^{-1} corresponds to overlapping –OH and N–H stretching vibrations, confirming the presence of hydroxyl and amine groups. These properties are crucial for filtering efficacy because of their involvement in hydrogen bonding and pH-dependent electrostatic interactions with suspended microplastics (Jeje and Edema, 2021; Lusiana et al., 2013). The C–H stretching peaks in the 2930–2960 cm^{-1} range further confirm the integrity of the polymer backbone.

Table 1. FTIR peak assignments of shrimp-shell chitosan extracts and their relevance to microplastic filtration

Peak region (cm^{-1})	Chitosan A	Chitosan B	Functional group assignment	Relevance to microplastic filtration	Reference
~3450	3451.25	3451.39	–OH / N–H stretching	Provides polar/amine functionalities supporting hydrogen bonding and pH-dependent electrostatic interactions with suspended particles	Jeje & Edema, 2021
2960–2850	2930.70	2962.20; 2933.53; 2892.12	C–H stretching	Confirms aliphatic polymer backbone	Lusiana et al., 2013
~1650	1651.26	1651.35	Amide I (C=O) and/or bound water contribution	Supports hydrophilicity/wettability, facilitating surface–particle contact during filtration	Cheung et al., 2015
1577–1569	1569.01	1576.65	Amide II (N–H bending)	Consistent with deacetylated chitosan and amine-related surface functionality (vs. neutral cellulose)	Hong et al., 2021
1205–1030	1204.63; 1157.09; 1072.44; 1030.94	1205.09; 1157.46; 1073.37; 1027.98	Polysaccharide fingerprint (C–O–C and C–O)	Confirms glycosidic/carbohydrate framework relevant for filter matrix formation	Rahman et al., 2022; Pathirana et al., 2023
~896	896.64	895.99	β-glycosidic linkage	Supports polysaccharide backbone identity/structural framework	Pathirana et al., 2023

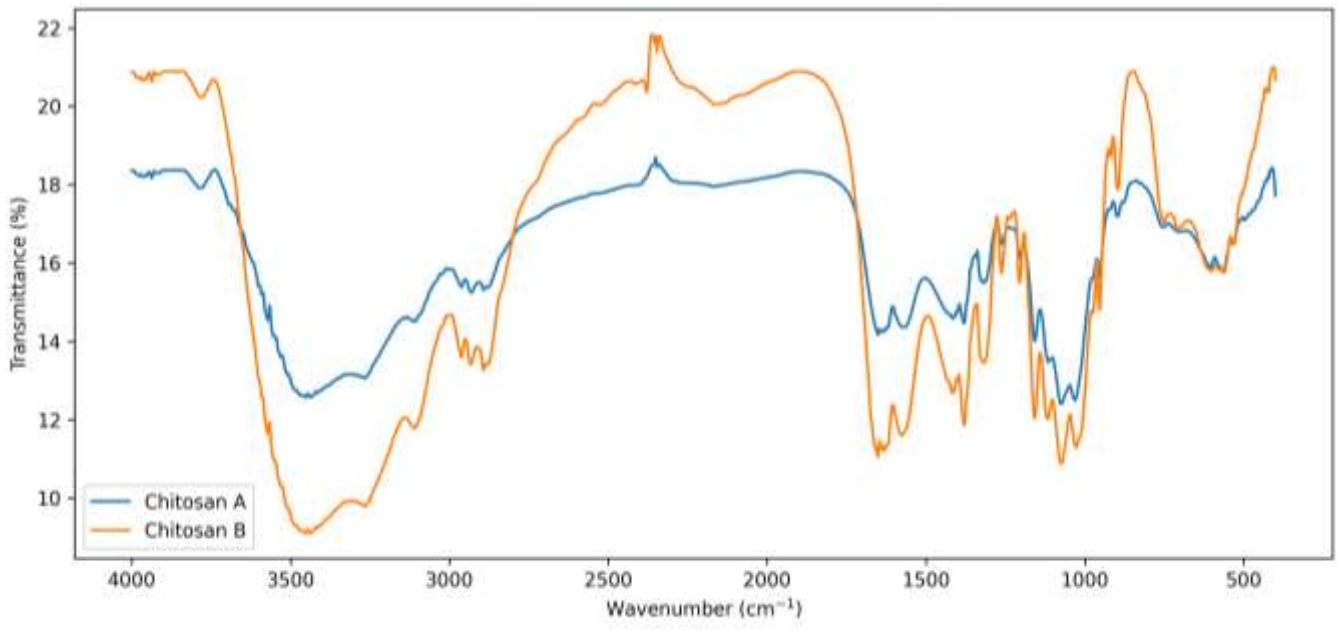

Figure 1. FTIR spectra of extracted shrimp-shell chitosan from two independent batches (Chitosan A and Chitosan B).

The C–H stretching vibrations observed in the 2930–2960 cm^{-1} region further support the presence of the polymer backbone. In the mid-wavenumber region, the band near 1650 cm^{-1} is typically assigned to amide I (C=O stretching) and contributions from bound water, both characteristic of hydrophilic biopolymers. The spectral characteristics may improve wettability and promote interaction between the filter surface and

suspended particles during filtration (Cheung et al., 2015). The amide II band at 1569–1577 cm^{-1} (N–H bending) is also consistent with deacetylated chitosan, indicating successful conversion from chitin and distinguishing chitosan from neutral cellulosic media, which lack amine-related spectral features (Hong et al., 2021).

The polysaccharide fingerprint region (1200–1000 cm^{-1}) offers further structural validation, indicating C–O–C and C–O vibrations linked to glycosidic bonds and the carbohydrate ring configuration. The β-glycosidic signal near 896 cm^{-1} offers further evidence of polysaccharide backbone integrity characteristic of chitosan (Pathirana et al., 2023). Collectively, these spectral characteristics confirm the identity of the extracted product as chitosan and establish a chemical basis for the particle retention behavior.

Beyond confirming characteristic chitosan functional groups, these FTIR results also demonstrate batch-to-batch consistency (Figure 1.). Spectra of Chitosan A and Chitosan B show aligned peak patterns across major bands—particularly at ~3450 cm^{-1} (–OH/N–H), ~1650 cm^{-1} (amide I), ~1569–1577 cm^{-1} (amide II), fingerprint region 1200–1000 cm^{-1}, and ~896 cm^{-1} (β-glycosidic). This spectral consistency confirms that the extraction and deacetylation process from shrimp shell waste produces reproducible chitosan, suitable as raw material for microplastic filtration performance testing.

Minor variations in peak intensity or bandwidth between batches are expected and may result from slight differences in degree of deacetylation, bound water content, or measurement technical factors (sample thickness, ATR contact quality). However, since key peak positions remain consistent, these differences do not alter the primary interpretation that the material exhibits chitosan chemical characteristics with polar/amine groups relevant for particle interactions during filtration.

Physical Characteristics of the Chitosan Filter Membrane

The chitosan-based filter was constructed as a thin, membrane-like sheet (about 0.2–0.5 mm thick) with a yellowish-cream hue, typical of deacetylated chitin-derived polymers. Unlike fibrous cellulose media with defined pore structures, the chitosan membrane formed a dense, crack-free matrix in its intact regions, suggesting that particle retention occurs primarily via surface-mediated mechanisms rather than size-exclusion filtration. The membrane conformed well to mold geometry, though peripheral edges showed slight unevenness and occasional microcracks due to differential shrinkage during solvent evaporation. The matte, non-glossy surface exhibited rough-granular texture from uniformly distributed fine chitosan particulates, contrasting with fibrous cellulose filter papers. Post-drying brittleness manifested as minor edge cracks, linked to non-uniform thickness and water evaporation shrinkage. Nevertheless, the central region of the membrane (approximately 70% of the surface area) remained compact and mechanically intact, supporting its suitability for vacuum-assisted filtration.

Figure 2. Macroscopic appearance of the fabricated chitosan membrane filter derived from shrimp-shell waste.

The chitosan membrane exhibited a dense polymeric matrix with micro-voids of 6–20 μm (median ~8 μm), alongside larger shrinkage-induced cracks (89–423 μm) that may contribute to preferential flow. This structure suggests retention occurs primarily via surface-mediated adhesion rather than size-exclusion. The membrane exhibited rapid wettability, consistent with the presence of hydrophilic –OH and $–NH_2$ functionalities as confirmed by FTIR (Table 1). In addition to serving as a physical barrier, these functional groups offer a mechanistic basis for particle adhesion and retention. This effect is particularly relevant for microplastics with organic coatings or biofilms, which display increased affinity for polar or charged surfaces compared to neutral cellulose-based media (Qin et al., 2024). Overall, these characteristics demonstrate the formation of a cohesive membrane suitable for filtration testing.

Macroscopic Visualization of Particle Deposition by Chitosan-Based Filters

Macroscopic retention patterns were evaluated across five media (chitosan membrane, coffee filter paper, Whatman No. 42, and their chitosan-coated

variants). A blank control using deionized water was processed under the same filtration protocol and showed no visible deposits, confirming that the observed residues originated from the microplastic suspension.

Uncoated commercial membranes (coffee filter paper and Whatman No. 42) exhibited fine, uniformly distributed "peppered" speckles across most of the active filtration area. This consistent deposition pattern aligns with passive retention mechanisms, chiefly physical interception and sieving within fibrous pore networks, alongside progressive surface loading (cake formation) characteristic of dead-end filtration as flow pathways become more resistive (Enfrin et al., 2020; Cohen et al., 2025). In this retention mode, capture sites are distributed throughout the filtration zone rather than concentrated in specific regions.

Conversely, pure chitosan membranes exhibited distinct, well-defined aggregates encircled by comparatively clear background areas, signifying an alternative retention mechanism. Along with mechanical sieving, surface-mediated adhesion drives localized particle consolidation at preferential sites. This mechanism is enhanced by –OH and $–NH_2$ groups (Table 1), which facilitate hydrogen bonding and pH-dependent electrostatic interactions (Risch et al., 2021; Putranto et al., 2023). Random particle interactions are transformed into self-amplifying deposition by initial anchor particles, which initiate cluster formation.

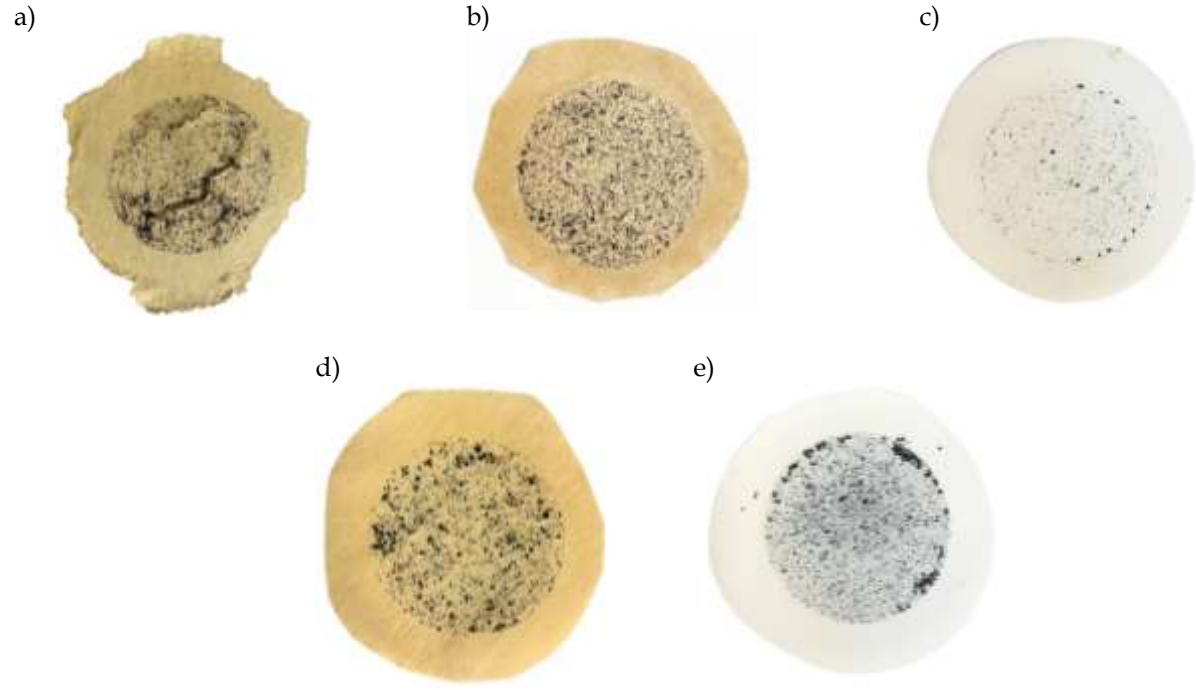

Figure 3. Macroscopic visualization of microplastic particle retention across different filtration media: (a) chitosan membrane filter, (b) chitosan-coated coffee filter, (c) chitosan-coated Whatman filter, (d) uncoated coffee filter, and (e) uncoated Whatman filter.

Chitosan-coated composites had intermediate characteristics, characterized by moderate clustering over a cellulose-like speckled substrate. The cellulose substrate allows for distributed mechanical interception, and the chitosan coating adds extra surface functionality that improves adhesion and deposition without producing the noticeable localized clumping seen in pure chitosan membranes. This hybrid pattern suggests a combined retention mechanism (Biopolymers Filtration Group, 2021). These contrasting deposition morphologies highlight key performance characteristics. While chitosan's localized aggregates improve retention of fine particles, they also increase local hydraulic resistance and mechanical stress, resulting in post-filtration brittleness and edge cracking that may facilitate preferential flow through defect propagation (Qin et al., 2024; Risch et al., 2021).

Filtration Rate

Filtration rate testing demonstrated significant throughput differences among the five media when filtering a fixed 50 mL microplastic suspension (Table 2). Coffee filter paper, among the cellulose-based options, achieved the fastest filtration (< 1 min; > 50 mL/min), which aligns with its larger pore size range (20–25 µm) and correspondingly low initial hydraulic resistance (Enfrin et al., 2020). On the other hand, Whatman No. 42 demonstrated the slowest filtration (± 7 min; 7.14

mL/min), which is in line with its denser pore network that limits flow through smaller channels and finer retention rating (~2.5 µm) (Enfrin et al., 2020; Balkenbusch et al., 2025). The chitosan membrane alone displayed intermediate throughput (± 5 min; 10 mL/min), situating its performance between the coarse and fine cellulose benchmarks.

Table 2. Filtration time and apparent filtration rate across filter media

Filter medium	Filtration time (± min)	Apparent filtration rate (mL/min)
Coffee filter paper	< 1	> 50
Chitosan-coated coffee filter	< 1	> 50
Chitosan membrane filter	± 5	10
Whatman No. 42	± 7	7.14
Chitosan-coated Whatman	± 7	7.14

Table 3. Size distribution of microplastics retained by different filter media

Filter medium	Minimum (µm)	Maximum (µm)
Coffee filter paper	0.447	1.919
Chitosan-coated coffee filter	0.719	3.517
Chitosan membrane filter	0.142	3.334
Whatman No. 42	0.107	1.708
Chitosan-coated Whatman No. 42	0.194	2.066

Chitosan-coated filter membranes generally retained the hydraulic properties of their cellulose substrates. The chitosan-coated coffee filter maintained a high throughput (> 50 mL/min), whereas the chitosan-coated Whatman filter exhibited performance comparable to the uncoated Whatman filter. This outcome suggests that the chitosan coating did not significantly increase bulk flow resistance under the tested conditions (Risch et al., 2021). However, filtration time is affected not only by the inherent pore structure but also by dynamic particle deposition during dead-end filtration. As retained particles accumulate, a deposit (cake) layer forms and increases hydraulic resistance. This effect is typically more pronounced in media with lower baseline permeability (Cohen et al., 2025; Balkenbusch et al., 2025).

The intermediate filtration rate of the chitosan membrane reflects its film-like structure and localized particle accumulation in the filtration zone. This deposition creates regions of high resistance, slowing flow compared to the more porous coffee filter paper, even if the entire surface is not blocked. FTIR analysis revealed the presence of –OH/–NH_2 functionalities (Table 1), which facilitate adhesion and retention of dispersed particles, including microplastics with organic coatings or biofilms that exhibit heightened affinity for polar or charged surfaces (Bhagat et al., 2024; Putranto et al., 2023).

Microscopic Visualization of Retained Particles

Microscopic examination (50–400× magnification) of filtration residues revealed distinct deposition features across media, underscoring correlations between surface morphology, retention patterns, and filtration-rate trends (Table 2). Differences in fiber openness, pore density, and surface chemistry likely influenced particle-media interactions and the resultant flow-deposition behavior (Enfrin et al., 2020).

Coffee filter paper displayed an open cellulose fiber matrix (20–25 µm interstices), in which residual microplastic particles were typically disseminated and situated individually between fibers, without creating a dense surface accumulation. This sparse retention pattern is associated with its elevated throughput (>50 mL/min; Table 2), as less hydraulic resistance facilitates swift flow while constraining conditions for consolidated surface loading (Al-Juboori et al., 2025). In contrast, the chitosan-coated coffee filter demonstrated more pronounced surface attachment, with particles accumulating as localized deposits and early-stage clusters on coated regions. This pattern signifies an extra contribution from chitosan-mediated adhesion, aligning with the presence of polar –NH_2/–OH functionalities that are lacking in uncoated cellulose substrates (Risch et al., 2021).

Uncoated Whatman No. 42 showed denser and more uniformly distributed deposits within its finer pore structure (~2.5 µm), with fine fragments often occupying much of the field of view. This higher deposit density corresponds to a longer filtration time (±7 min; Table 2), indicating heightened surface loading and augmented resistance during dead-end filtration in denser material (Balkenbusch et al., 2025). The chitosan-coated Whatman exhibited an intermediate morphology, characterized by a retained tightly packed cellulose framework and a chitosan layer that partially obscured pore openings. Retained particles manifested as distinct dark granules and luminous or transparent fragments within the fiber matrix, signifying retention through mechanical sieving and supplementary surface adhesion from chitosan (Putranto et al., 2023). The production of large aggregates was less evident, probably because to the dense substrate structure.

The chitosan membrane showed a contrasting pattern, with retained residues appearing as prominent clusters or aggregates firmly attached to the granular membrane matrix, resulting in a clumped deposition

pattern consistent with macroscopic observations. This clustering indicates that retention on chitosan entails not only pore-scale sieving but also surface-mediated adhesion and localized particle agglomeration. These processes may be especially relevant for smaller fragments that can escape size-exclusion capture (Bhagat et al., 2024; Risch et al., 2021). This effect is mechanistically possible due to the cationic nature of chitosan. Protonated amine groups ($-NH_3^+$) may adsorb onto negatively charged microplastic surfaces depending on the solution pH, while polymer chain bridging can destabilize suspended particles and facilitate aggregation, with intra-aggregate hydrogen bonding potentially enhancing aggregate stability (Putranto et al., 2023; Risch et al., 2021)

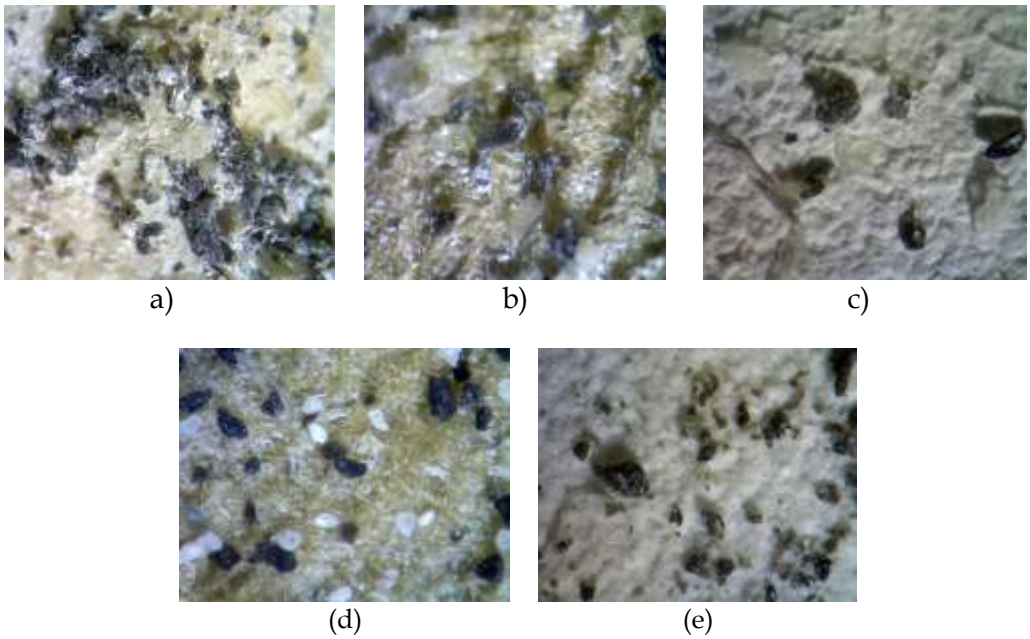

Figure 4. Microscopic visualization of microplastic particle retention across different filtration media: (a) chitosan membrane filter, (b) chitosan-coated coffee filter, (c) chitosan-coated Whatman filter, (d) uncoated coffee filter, and (e) uncoated Whatman filter.

Size Distribution of Retained Microplastics Across Filter Media

Morphometric examination of residual microplastic residues revealed specific minimum and maximum size ranges within the evaluated filtration media (Table 3). Chitosan-based membran filter demonstrated a wider range of retained particle sizes than uncoated cellulose. The chitosan-coated coffee filter exhibited the greatest maximum maintained size (3.517 µm), succeeded by the independent chitosan membrane (3.334 µm), both exceeding the maxima recorded for uncoated cellulose media (coffee filter: 1.919 µm; Whatman No. 42: 1.708 µm). Very low minimum values were also detected across several media (e.g., Whatman: 0.107 µm; chitosan membrane: 0.142 µm), suggesting that retention under the existing dead-end filtration conditions was affected by both nominal pore attributes and dynamic surface phenomena that occur during operation (Enfrin et al., 2020). These broader size retention ranges in chitosan-containing media are consistent with the surface-mediated adhesion and aggregate growth mechanisms described in the preceding microscopic analysis, further supporting chitosan's role beyond passive sieving.

Consistent with these findings, the chitosan-coated Whatman filter exhibited only a modest increase in maximum retained size (2.066 µm compared to 1.708 µm for uncoated Whatman), presumably attributable to the limitations of the denser substrate structure. The more porous configuration of the coffee-filter support facilitated an enhanced level of surface-driven deposition and aggregate formation in the chitosan-coated format (Balkenbusch et al., 2025). These size-distribution patterns support the macroscopic and microscopic evidence that chitosan modifies filtration behavior, shifting it from primarily size-exclusion capture to include additional surface-mediated retention mechanisms capable of retaining both larger fragments and very fine particles under the tested conditions.

Overall, this proof-of-concept study demonstrates that chitosan derived from shrimp shells can be produced and functions as an effective microplastic filtration medium. The chitosan membrane demonstrates unique retention characteristics and collects a wider spectrum of microplastics compared to

uncoated cellulose controls. The primary innovation is the development of a waste-to-resource chitosan membrane filter platform that can be used as either a standalone membrane or a coating. This platform allows retention beyond passive filtration by promoting surface-mediated deposition and aggregation. However, key limitations include the use of a controlled microplastic suspension rather than actual wastewater, the absence of quantitative removal metrics and comprehensive size-distribution data, and the post-filtration brittleness of the chitosan membrane. Future investigations should evaluate removal efficiency and particle size distributions under actual settings, and refine membrane formulation to enhance mechanical durability while preserving retention performance.

Conclusion

Shrimp shell waste was successfully converted into chitosan, as confirmed by FTIR analysis, and fabricated into functional filtration media for microplastic, evidenced by distinct macroscopic clumping, microscopic aggregation, and expanded size retention (max 3.517 µm vs. cellulose 1.919 µm). Compared to commercial filter membrane with cellulose filters, chitosan-containing systems, both pure granular membrane and cellulose coatings, demonstrated surface-mediated retention pathways via cationic flocculation alongside mechanical interception, while filtration throughput remained substrate-dominated. These findings establish a low-cost, bio-based proof-of-concept for chitosan floc-filtration technology, providing a foundation for quantitative validation of removal and mechanical optimization toward practical deployment. The demonstrated feasibility of this waste-to-resource approach suggests promising potential for integration into laboratory-scale and pilot-scale wastewater treatment systems, particularly as a low-cost pre-treatment or modular filtration unit.

Acknowledgments
The authors gratefully acknowledge all Center of Marine Ecology and Biomonitoring for Sustainable Aquaculture (Ce-MEBSA) team members for their assistance with experimental and data analyses.

Author Contributions
Conceptualization, R.S.T., S.A.Y., F.R.P., A.S.P.P.; Methodology, R.S.T., A.S.P.P.; Data curation, R.S.T., D.H., L.I., S.A.Y., F.R.P.; Writing – original draft preparation, R.S.T., S.A.Y., F.R.P.; Writing – review and editing, R.S.T., D.H.; Supervision, R.S.T., S.P.P.,A.S.P.P. . All authors have read and agreed to the published version of the manuscript.

Funding
This research received no external funding

Conflicts of Interest
The authors declare no conflict of interest.

References

Amirah Mohd Napi, N. nor, Ibrahim, N., Adli Hanif, M., Hasan, M., Dahalan, F. A., Syafiuddin, A., & Boopathy, R. (2023). Column-based removal of high concentration microplastics in synthetic wastewater using granular activated carbon. *Bioengineered*, *14*(1). https://doi.org/10.1080/21655979.2023.2276391

Balkenbusch, C., Glienke, J., Wu, Y., Almuhtaram, H., & Andrews, R. C. (2025). Microplastic removal across ten drinking water treatment facilities and distribution systems. *npj Clean Water*, *8*, 103. https://doi.org/10.1038/s41545-025-00531-w

Badawi, A. K., Hassan, R., & Ismail, B. (2025). Sustainable coagulative removal of microplastic from aquatic systems: recent progress and outlook. *RSC Advances*, *15*(31), 25256–25273. https://doi.org/10.1039/D5RA04074D

Bhagat, K., Doussiemo, D. R. B., Mushro, N., Rajwade, K., Kumar, A., Apul, O., & Perreault, F. (2024). Effect of biofouling on the sorption of organic contaminants by microplastics. *Environmental Toxicology and Chemistry*, *43*(9), 1973–1981. https://doi.org/10.1002/etc.5938

Bavel, N., Issler, T., Pang, L., Anikovskiy, M., & Prenner, E. (2023). A simple method for synthesis of chitosan nanoparticles with ionic gelation and homogenization. Molecules, 28(11), 4328. https://doi.org/10.3390/molecules28114328

Biopolymers Filtration Group. (2021). Biopolymer-based filtration materials. *Polymers*, 13(9), 1384. **https://doi.org/10.3390/polym13091384**

Cheung, R., Ng, T., Wong, J., & Chan, W. (2015). Chitosan: An Update on Potential Biomedical and Pharmaceutical Applications. Marine Drugs, 13(8), 5156-5186. https://doi.org/10.3390/md13085156

Cohen, N., Edery, Y., & Radian, A. (2025). Pore-scale insights into microplastic fiber transport and retention in porous media. *Environmental Science & Technology*, *59*(50), 27657–27667. https://doi.org/10.1021/acs.est.5c12359

Davis, E. and Raja, S. (2020). Sources and impact of microplastic pollution in indian aquatic ecosystem: a review. Current World Environment, Special Issue(1). https://doi.org/10.12944/cwe.15.special-issue1.01

Enfrin, M., Dumée, L. F., & Lee, J. (2020). Nano/microplastics in water and wastewater treatment processes – Origin, impact and potential solutions. *Water Research*, 161, 621-638. https://doi.org/10.1016/j.watres.2019.06.049

Hong, G., Yu, T., Lee, H., & Ma, C. (2021). Using Rice Bran Hydrogel Beads to Remove Dye from Aqueous Solutions. Sustainability, 13(10), 5640. https://doi.org/10.3390/su13105640

Jeje, O. and Edema, O. (2021). Adsorption of Colour Pigments from Palm Kernel Oil onto Biopolymer Prepared from Periwinkle Shell Waste. International Journal of Biochemistry Research & Review, 51-62. https://doi.org/10.9734/ijbcrr/2021/v30i930290

Kamani, H., Ghayebzadeh, M., & Ganji, F. (2024). Tracking and risk assessment of microplastics in a wastewater treatment plant. Water and Environment Journal, 38(4), 613-627. https://doi.org/10.1111/wej.12949

Karbalaei, S., Hanachi, P., Walker, T., & Cole, M. (2018). Occurrence, sources, human health impacts and mitigation of microplastic pollution. Environmental Science and Pollution Research, 25(36), 36046-36063. https://doi.org/10.1007/s11356-018-3508-7

Lapointe, M., Farner, J., Hernandez, L., & Tufenkji, N. (2020). Understanding and improving microplastic removal during water treatment: impact of coagulation and flocculation. Environmental Science & Technology, 54(14), 8719-8727. https://doi.org/10.1021/acs.est.0c00712

Lusiana, R., Siswanta, D., Mudasir, M., & Hayashita, T. (2013). The influence of pva.cl.citric acid/chitosan membrane hydrophicility on the transport of creatinine and urea. Indonesian Journal of Chemistry, 13(3), 262-270. https://doi.org/10.22146/ijc.21286

Nawaz, F., Islam, Z., Ghori, S., Bahadur, A., Ullah, H., Ahmad, M., … & Khan, G. (2025). Microplastic and nanoplastic pollution: assessing translocation, impact, and mitigation strategies in marine ecosystems. Water Environment Research, 97(2). https://doi.org/10.1002/wer.70032

Pathirana, M., Dissanayake, N., Wanasekara, N., Mahltig, B., & Nandasiri, G. (2023). Chitosan-Graphene Oxide Dip-Coated Polyacrylonitrile-Ethylenediamine Electrospun Nanofiber Membrane for Removal of the Dye Stuffs Methylene Blue and Congo Red. Nanomaterials, 13(3), 498. https://doi.org/10.3390/nano13030498

Picos-Corrales, L., Sarmiento-Sánchez, J., Ruelas-Leyva, J., Crini, G., Hermosillo-Ochoa, E., & Gutierrez-Montes, J. (2020). Environment-friendly approach toward the treatment of raw agricultural wastewater and river water via flocculation using chitosan and bean straw flour as bioflocculants. Acs Omega, 5(8), 3943-3951. https://doi.org/10.1021/acsomega.9b03419

Putranto, P. A., Khoironi, A., & Baihaqi, R. A. (2023). Optimisation of chitosan as a natural flocculant for microplastic remediation. *Journal of Emerging Science and Engineering*, *1*(2), 44–50. https://doi.org/10.61435/jese.2023.7

Qin, Y., Tu, Y., Chen, C., et al. (2024). Biofilms on microplastic surfaces and their effect on pollutant adsorption in the aquatic environment. *Journal of Material Cycles and Waste Management*, *26*, 3303–3323. https://doi.org/10.1007/s10163-024-02066-7

Rajendran, S., Al-Samydai, A., Palani, G., Trilaksana, H., Sathish, T., Giri, J., … & Nasri, F. (2025). Replacement of petroleum based products with plant-based materials, green and sustainable energy—a review. Engineering Reports, 7(4). https://doi.org/10.1002/eng2.70108

Risch, P., & Adlhart, C. (2021). A chitosan nanofiber sponge for oyster-inspired filtration of microplastics. *ACS Applied Polymer Materials*, *3*(9), 4685–4694. https://doi.org/10.1021/acsapm.1c00799

Sanjeev, N. and Manjunath, S. (2025). Nanotechnology-based approaches for the removal of microplastics from wastewater: a comprehensive review. Beilstein Journal of Nanotechnology, 16, 1607-1632. https://doi.org/10.3762/bjnano.16.114

Sethia, P., Nandhini, D., & Amutha, S. (2024). Effects of marine microplastic on marine life and the food webs – a detailed review. Marine Ecology, 45(5). https://doi.org/10.1111/maec.12819

Talvitie, J., Mikola, A., Koistinen, A., & Setälä, O. (2017). Solutions to microplastic pollution – Removal of microplastics from wastewater effluent with advanced wastewater treatment technologies. *Water Research*, 123, 401–407. https://doi.org/10.1016/j.watres.2017.07.005

Thathsarani, N., Najafi, M., Khiadani, M., Azhar, M. R., & Zargar, M. (2025). Integrated chitosan-based coagulation and microbubble pre-treatment for improved microplastic fibre removal from water. *Science of the Total Environment*, *1009*, 181039. https://doi.org/10.1016/j.scitotenv.2025.181039

Uogintė, I., Pleskytė, S., Pauraitė, J., & Lujanienė, G. (2022). Seasonal variation and complex analysis of microplastic distribution in different wwtp treatment stages in lithuania. Environmental Monitoring and Assessment, 194(11). https://doi.org/10.1007/s10661-022-10478-x

Wang, H., Liu, X., & Zhao, P. (2025). Advances in chitin and chitosan-based materials for microplastics treatment. Environmental Research, 256, 118948. https://pubmed.ncbi.nlm.nih.gov/40912793